Vol. 24(2):135-146 | Ocean and Polar Research | June 2002

Article

Simulation of the Mixed Layer in the Western Equatorial Pacific Warm Pool

Chan Joo Jang*[1] and Yign Noh[2]

[1]*Coastal and Harbor Engineering Research Laboratory, KORDI*
Ansan P.O. Box 29, Seoul 425-600, Korea
[2]*Department of Atmospheric Sciences, Yonsei University*
Seoul 120-749, Korea

Abstract : The upper ocean in the western equatorial Pacific warm pool during TOGA-COARE IMET IOP was simulated using a one-dimensional turbulence closure ocean mixed-layer model, which considered recent observations, such as the remarkable enhancement of turbulent kinetic energy near the ocean surface. The shoaling/deepening of the mixed layer and warming/cooling subsurface water in the model were in reasonable agreement with the observations. There was a significant improvement in simulating the cooling trend of the sea surface temperature under a westerly wind burst with heavy rainfall over previous simulations using bulk mixed-layer models. By contrast, the simulated sea surface salinity (SSS) departed significantly from the observed SSS, especially during a westerly burst and the subsequent restratification period, which might be due to 3-D control processes, such as downwelling/upwelling or advection.

Key words : mixed-layer model, warm pool, cooling trend, SST, SSS.

1. Introduction

The western equatorial Pacific warm pool, which is characterized by a mean sea surface temperature (SST) exceeding 28°C with a strong air-sea interaction, provides a major driving force for the global atmospheric circulation: SST variation on the order of 1°C in this region can result in dramatic shifts in global weather patterns (Palmer and Mansfield 1984). Therefore, understanding the processes controlling warm pool SST variability is crucial in studies of global climate variability.

The SST in the warm pool region is relatively homogeneous in comparison with other regions of the equatorial Pacific. Hence, it has been assumed that one-dimensional models should be able to simulate temperature reasonably well in this region, although heat advection or entrainment can be a dominant mechanism in the heat balance before and during a westerly wind burst (Cronin and McPhaden 1997). In particular, Anderson *et al.* (1996) showed that a one-dimensional model was appropriate for most time periods due to negligible horizontal advection of heat during the Tropical Ocean Global Atmosphere (TOGA) Coupled Ocean-Atmosphere Response Experiment (COARE). Therefore, various authors have used one-dimensional mixed-layer models to simulate diurnal and intraseasonal variation in SST in the warm pool during the TOGA-COARE Intensive Observation Period (IOP) (Anderson *et al.* 1996; Cronin and McPhaden 1997; Sui *et al.* 1997; Li *et al.* 1998).

Anderson *et al.* (1996) employed a one-dimensional mixed-layer model similar to the dynamic instability model of Price *et al.* (1986) to examine the local response of the mixed layer in the warm pool to surface forcing using TOGA-COARE IOP observations. They were able to reproduce the evolution of the upper ocean, and found that the freshwater flux limits mixed layer depth, thereby altering the amplitude of the simulated SST fluctuations. Sui *et al.* (1997) showed that the vertical distribution of

*Corresponding author. E-mail : cjjang@kordi.re.kr

solar penetration is crucial for the evolution of the mixed-layer temperature using the one-dimensional bulk mixed-layer model of Adamec *et al.* (1981). They also found that the accumulation effect of diurnal mixing cycles (solar heating/nocturnal cooling) is important in the evolution of the mixed-layer temperature and depth on an intraseasonal scale. Li *et al.* (1998) used the same mixed-layer model as Sui *et al.* (1997), and suggested that the entrainment process in the model remarkably reduces the biased freshening trend during a westerly wind burst by entraining saline water into the mixed layer.

Although the basic diurnal and intraseasonal variations in the upper layer in the warm pool have been well simulated, there are still significant differences between simulations and observations (Li *et al.* 1998). For example, the simulated diurnal amplitude of the SST is smaller than observed, and the temperature decreases more slowly in simulations than in observations during a westerly wind burst.

Most simulations so far have adopted bulk mixed-layer models, which ignore the production of turbulent kinetic energy by vertical velocity shear. As a common shortcoming, the bulk models generate a very weak cooling trend for SST under a westerly wind burst with heavy rainfall (Anderson *et al.* 1996; Sui *et al.* 1997; Li *et al.* 1998). Clayson and Kantha (1999) used a one-dimensional mixed-layer model of second order turbulence closure, instead of a bulk model, to simulate TOGA-COARE IOP observations. Good qualitative agreement was achieved with the observed cooling trend in SST, but the simulation covered a limited portion of the IOP, and not the entire set of observations.

Therefore, this study simulated the upper ocean in the western Pacific warm pool during the IOP using a new turbulence closure mixed-layer model to improve simulation of SST, focusing on the cooling trend of SST during a westerly wind burst. The new ocean mixed-layer model (OMLM) based on Noh and Kim (1999) is a second order turbulence closure model that uses eddy diffusivity, but it produces a well-mixed layer, even under a stabilizing heat flux, consistent with observations and bulk-type OMLMs (Niiler and Kraus 1977). Most other OMLMs using eddy diffusivity lead to strong stratification and shear near the surface under a stabilizing heat flux (Mellor and Yamada 1982).

We begin by describing the mixed-layer model in Section 2. Section 3 presents experiments, and the observed characteristics of surface forcing during the TOGA-COARE IOP. The results of the model are compared with observations in Section 4 and the results are summarized and conclusions are drawn in Section 5.

2. Mixed-layer model

The mixed-layer model used here is based on Noh and Kim (1999), and has been recently modified to include freshwater flux and solar penetration. The equations governing the horizontal mean velocity U and V, the mean temperature T, the mean salinity S, and the mean turbulent kinetic energy (TKE) E in a horizontally homogeneous ocean boundary layer under the Boussinesq approximation can be written as follows (Phillips 1977; Martin 1985):

$$\frac{\partial U}{\partial t} = -\frac{\partial}{\partial z}\overline{uw} + fV, \tag{1}$$

$$\frac{\partial V}{\partial t} = -\frac{\partial}{\partial z}\overline{vw} - fU, \tag{2}$$

$$\frac{\partial T}{\partial t} = -\frac{\partial}{\partial z}\overline{wT''} + \frac{1}{\rho_0 c_p} Q_R \frac{\partial I}{\partial z}, \tag{3}$$

$$\frac{\partial S}{\partial t} = -\frac{\partial}{\partial z}\overline{wS''}, \tag{4}$$

$$\frac{\partial E}{\partial t} = -\frac{\partial}{\partial z}\overline{w\left(\frac{p}{\rho_0} + E\right)} - \overline{uw}\frac{\partial U}{\partial z} - \overline{vw}\frac{\partial V}{\partial z} - \overline{bw} - \varepsilon. \tag{5}$$

Here, t is the time, and z is the vertical coordinate, which is positive downward from the sea surface, u, v, and w are the horizontal and vertical components of fluctuating velocity, respectively, Q_R is the absorbed solar radiation at the ocean surface, I is the fraction of the solar radiation that penetrates to a given depth, T' and S' are the fluctuating temperature and salinity. b is the fluctuating buoyancy ($= -g(\rho - \rho_0)/\rho_0$) involving the reference density of seawater ρ_0 and gravity g, c_p is the specific heat of seawater, f is the Coriolis parameter, ρ and p are the fluctuation of density and pressure, respectively, and ε is the dissipation rate of TKE.

Following Paulson and Simpson (1977), the penetration of solar radiation is parameterized by

$$I(z) = Re^{-z/\gamma_1} + (1-R)e^{-z/\gamma_2} \tag{6}$$

where R is an empirical constant, and γ_1 and γ_2 are attenuation lengths. The first term on the right hand side of (6) represents the red part of the spectrum associated with an e-folding depth of approximately 1 m, and the second term represents the blue-green part associated

with an e-folding depth of about 15 m (Jerlov 1968).

The first four terms on the right-hand side of (5) represent the flux of TKE, the production of TKE by the mean velocity shear, and the production or decay of TKE by the buoyancy flux, respectively. Introducing the eddy diffusivity, equations (1)-(5) above can be rewritten as follows:

$$\frac{\partial U}{\partial t} = \frac{\partial}{\partial z}\left(K\frac{\partial U}{\partial z}\right) + fV, \tag{7}$$

$$\frac{\partial V}{\partial t} = \frac{\partial}{\partial z}\left(K\frac{\partial V}{\partial z}\right) - fU, \tag{8}$$

$$\frac{\partial T}{\partial t} = \frac{\partial}{\partial z}\left(K_H\frac{\partial T}{\partial z}\right) + \frac{1}{\rho_0 c_p}Q_R\frac{\partial I}{\partial z}, \tag{9}$$

$$\frac{\partial S}{\partial t} = \frac{\partial}{\partial z}\left(K_H\frac{\partial S}{\partial z}\right) \tag{10}$$

$$\frac{\partial E}{\partial t} = \frac{\partial}{\partial z}\left(K_E\frac{\partial E}{\partial z}\right) + K\left[\left(\frac{\partial U}{\partial z}\right)^2 + \left(\frac{\partial V}{\partial z}\right)^2\right] + K_H\frac{\partial B}{\partial z} - \varepsilon, \tag{11}$$

Here, B is the mean buoyancy. The eddy viscosity K, the eddy diffusivity K_H, and the eddy diffusivity of TKE K_E are modeled as

$$K = S_M ql, \tag{12}$$

$$K_H = S_H ql, \tag{13}$$

$$K_E = S_E ql, \tag{14}$$

where q is the root mean square (rms) velocity of the turbulence ($= (2E)^{1/2}$) and l is the length scale of the turbulence. The dissipation rate is calculated using

$$\varepsilon = Cq^3 l^{-1}. \tag{15}$$

Under neutral stratification, the constants are taken as $S_M = 0.39$ ($= S_0$), Pr ($= S_M/S_H$) $= 0.8$, σ ($= S_M/S_E$) $=1.95$, and $C = 0.06$ ($= C_0$), which are the same as in the Mellor-Yamada (1982) model. Here, the subscript 0 represents the values of the empirical coefficients in the absence of stratification. Similar values have also been used in other models: for example, $S_0 = 0.33$, $Pr = 0.8$, $\sigma = 1.37$, and $C_0 = 0.04$ by Davies and Jones (1988).

The boundary conditions at the sea surface ($z = 0$) are given by

$$K\frac{\partial U}{\partial z} = \frac{\tau_x}{\rho_0}, \tag{16}$$

$$K\frac{\partial V}{\partial z} = \frac{\tau_y}{\rho_0}, \tag{17}$$

$$K_H\frac{\partial T}{\partial z} = \frac{1}{\rho_0 c_p}Q_R, \tag{18}$$

$$K_H\frac{\partial S}{\partial z} = -S_r[P - E] \tag{19}$$

$$K_E\frac{\partial E}{\partial z} = mu_*^3, \tag{20}$$

where τ_x and τ_y are the wind stresses in the east-west and north-south directions, respectively, u_* is the frictional velocity defined by $u_*^2 = \tau/\rho_0$ involving wind stress $\tau = [\tau_x^2 + \tau_y^2]^{1/2}$, and m is an empirical constant determining the TKE flux at the sea surface. No net fluxes of TKE, buoyancy, and momentum are assumed at the model bottom ($z = 100$ m).

The length scale l is given by

$$l = \frac{\kappa[z + z_0]}{1 + \kappa[z + z_0]/h}, \tag{21}$$

where z_0 is the roughness length scale, h is the mixed-layer depth (MLD), and κ is von Kármán constant (=0.4).

Equations (7)-(19) are typical for second order turbulence closure model. However, the important differences between the new OMLM and the Mellor and Yamada model lie in the parameterization of the surface TKE flux and in the effect of stratification (Noh and Kim 1999).

The boundary condition for TKE is given by (20). Based on Craig and Banner's analysis (1994) of recent observations of the upper ocean, Noh and Kim (1999) assumed the values $m = 100$ and $z_0 = 1$ m for (20) and (21). These values were chosen to represent intensive mixing near the sea surface. In this case the relevant Richardson number, which is used to represent the effects of stratification, should be determined in terms of TKE itself rather than the mean velocity shear, because the TKE flux plays an important role in TKE production. Therefore, the TKE Richardson number defined by

$$Rt = (Nl/q)^2, \tag{22}$$

must be used instead of the flux Richardson number. Here, N is the buoyancy frequency. In this case we can parameterize the effects of stratification as

$$S_M/S_0 = (1 + \alpha Rt)^{-1/2}, \tag{23}$$

$$C/C_0 = (1 + \alpha Rt)^{1/2}, \tag{24}$$

while maintaining the proportionality of S_H and S_E to S_M. Here, α is an empirical constant, which was set as 120 following Noh and Kim (1999). A uniform mixed layer

is enforced during convection, which means $K_M = K_H = \infty$ whenever $Rt < 0$. However, the vertical transfer of TKE is assumed to be unaffected by convection, based on scaling analysis (Noh and Kim 1999).

The OMLM successfully predicted the evolution of the vertical profiles of both the temperature and the turbulence structure of the mixed layer, as well as the SST (Noh and Kim 1999). The new OMLM also simulated the formation of a diurnal thermocline realistically, which remain as one of the most difficult part in most OMLMs (Noh 1996).

The model parameters (m and z_0) were modified to simulate the mixed layer in the warm pool during TOGA-COARE IOP, which is presented in the following section.

3. Experiment and surface forcing

The model was initialized using the observed temperature and salinity on 1 Nov. 1992 from the Woods Hole Oceanographic Institution (WHOI) surface mooring deployed in the center of the Intensive Flux Array (IFA) at 156°E, 1.8°S during the TOGA COARE IOP. The model was forced by the hourly surface heat flux and the freshwater flux from the updated processed Improved Meteorological (IMET) Surface Mooring buoy (Weller and Anderson 1996). The evaporation rate (E) was calculated from the latent heat flux(Q_{LAT}) as follows (Barnier 1998):

$$E = \frac{Q_{LAT}}{\rho_w L}, \tag{25}$$

where ρ_w is the density of seawater, and L is the latent heat of vaporization. Consequently, the evaporation flux will be affected by uncertainties in the latent heat flux calculation. The total depth of the model is 100 m. The vertical resolution is 0.2 m and the time step is 1 sec.

It has been shown that the vertical distribution of solar radiation $I(z)$ is crucially important in the temperature evolution of the mixed layer in the warm pool (Anderson *et al.* 1996; Sui *et al.* 1997). After sensitivity tests using different values of γ_1 and γ_2, we found that the following values were the most appropriate for our model simulation in terms of SST: $\gamma_1 = 0.6$ m and $\gamma_2 = 20.0$ m. These empirical attenuation coefficients correspond to water type 1A in the classification of Jerlov (1968). Anderson *et al.* (1996) used the same water type.

To approximate the effect of frictional velocity on the surface TKE flux and the roughness length scale, the boundary conditions for the TKE flux and roughness length scale were modified as follows:

$$m = m_0 \left(1 - e^{-au_*^2}\right) \quad m_0 = 100 \quad a = 10^4, \tag{26}$$

$$z_0 = z_0 \left(1 - e^{-bu_*^2}\right) \quad z_0 = 1 \quad b = 5 \times 10^3. \tag{27}$$

The rationale for this is as follows. The frictional velocity (Fig. 1c) at the IMET buoy is weak (below 0.01 ms^{-1}) most of the time. As a result, the surface mixing by wave breaking or Langmuir circulation due to wind is expected to be weak. Consequently, their effects on m and z_0, are parameterized as an exponential function of the frictional velocity.

The observed surface forcings at the IMET buoy during the simulation period (1 Nov. 1992-3 Mar. 1993) are shown in Fig. 1. Fig. 2 shows the four components of the net heat flux: net solar radiation, latent heat flux, sensible heat flux, and net longwave radiation. A positive heat flux corresponds to heating of the ocean surface. From Fig. 2, it is evident that net solar radiation and latent heat flux are the major contributors to the net heat flux. The variation in the surface forcing observed during the IOP has been discussed in previous studies (Weller and Anderson 1996; Anderson *et al.* 1996; Sui *et al.* 1997). We focus on periods of westerly wind bursts with heavy rainfall and subsequent restratification. Three consecutive westerly wind bursts accompanying heavy rainfall were observed from Dec. 1992 through early Jan. 1993. During these events, a small amount of solar radiation and a large latent heat flux, together with a large freshwater flux, led to cooling of the ocean surface and a consequent decrease in SST. During the restratification period (5-15 Jan. 1993) immediately after the period of westerly wind bursts, strong solar heating and weak latent cooling gave rise to strong heating of the ocean, leading to restratification of the upper ocean (Fig. 1c) and a consequent rapid rise in SST. While the SST directly corresponds to the variation in the net heat flux most of the time, the variation in the sea surface salinity (SSS) at 2 m (Fig. 1e) does not match the variation in the freshwater flux well. For example, the SSS does not tend to decrease on average during heavy rainfall (Dec. 1992 through early Jan. 1993).

4. Results

Temporal variations in the simulated SST and subsurface temperature are shown in Fig. 3, together with observed values. Note that the observed SST is defined as the surface temperature at 0.45 m, while the model SST is

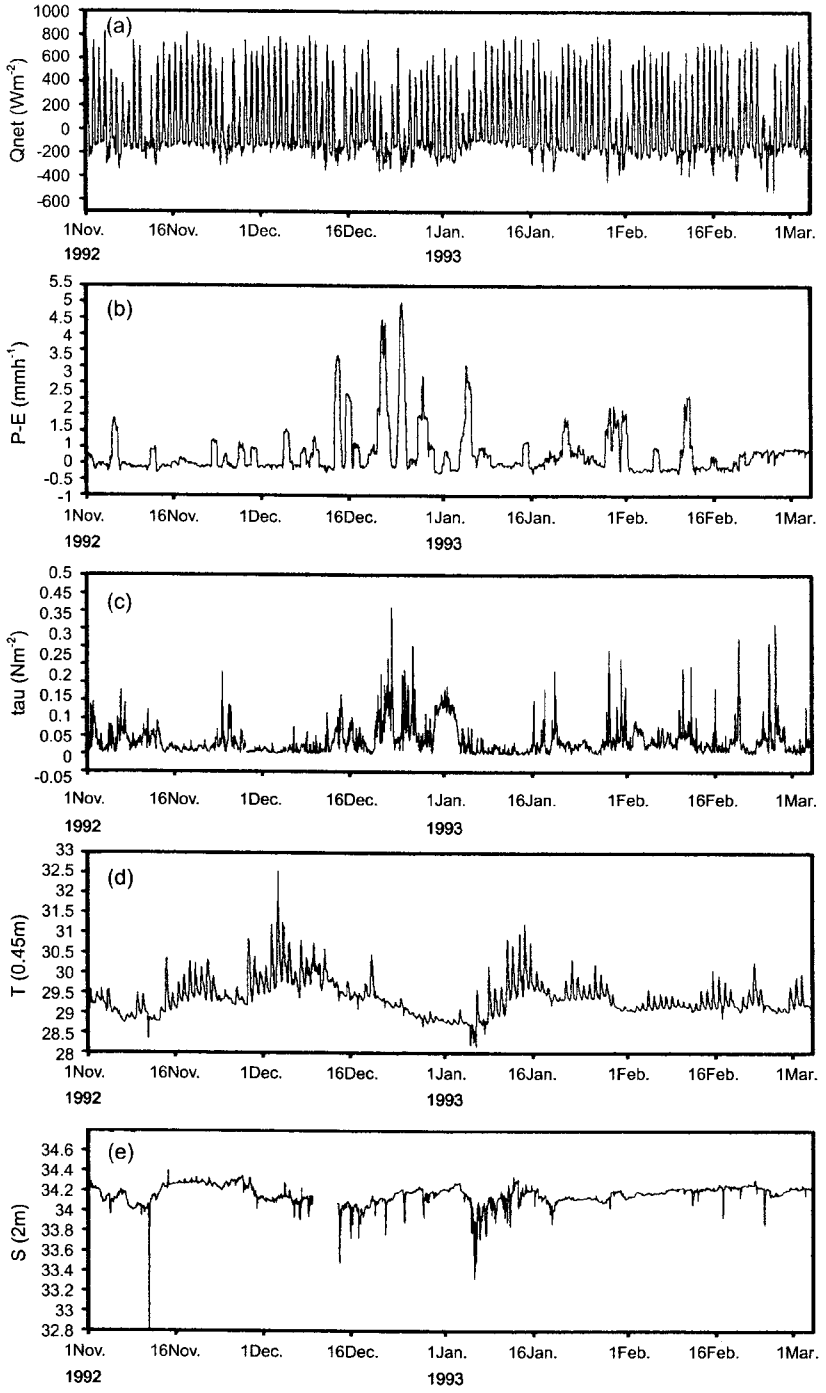

Fig. 1. Time series of hourly surface forcing, SST and SSS observed at IMET buoy during TOGA-COARE IOP: (a) net heat flux, (b) freshwater flux, (c) wind stress, (d) SST, and (e) SSS. Positive values in heat and freshwater flux are gains for the ocean. Note that there is period of SSS data missing.

taken to be the temperature at 1 m due to the discrete model grid points.

The calculated MLDs from both the model and observations are also shown in Fig. 3b. Various criteria have been used to define the MLD in the warm pool region for the observed hydrography during the IOP

(Anderson *et al.* 1996; Sui *et al.* 1997; Li *et al.* 1998). For example, Sui *et al.* (1997) defined the MLD using the temperature difference from surface values, while Li *et al.* (1998) defined the MLD using the density difference from surface values. These criteria employ two methods, one based on a maximum vertical gradient and the other on the difference from the sea surface value. Anderson *et al.* (1996) summarized the MLD criteria used by several authors (Table 2 in Anderson *et al.* 1996).

Like Sui *et al.* (1997), we define the MLD as the depth at which the temperature is 0.2°C lower than the SST. Therefore, the MLD defined in this study has the same meaning as the depth of the isothermal layer. Anderson *et al.* (1996) estimated the MLD using the difference from surface values using the vertical profiles of temperature, salinity, and potential density observed during the IOP. They found that the IOP-mean MLD from temperature profiles is only 5 m smaller than that from density profiles. Therefore, the MLD as defined in this study should not differ significantly from the isopycnal depth on average.

The simulated MLD and SST displays both intraseasonal and diurnal variation. The simulated intraseasonal variation is characterized by two cycles of surface warming/

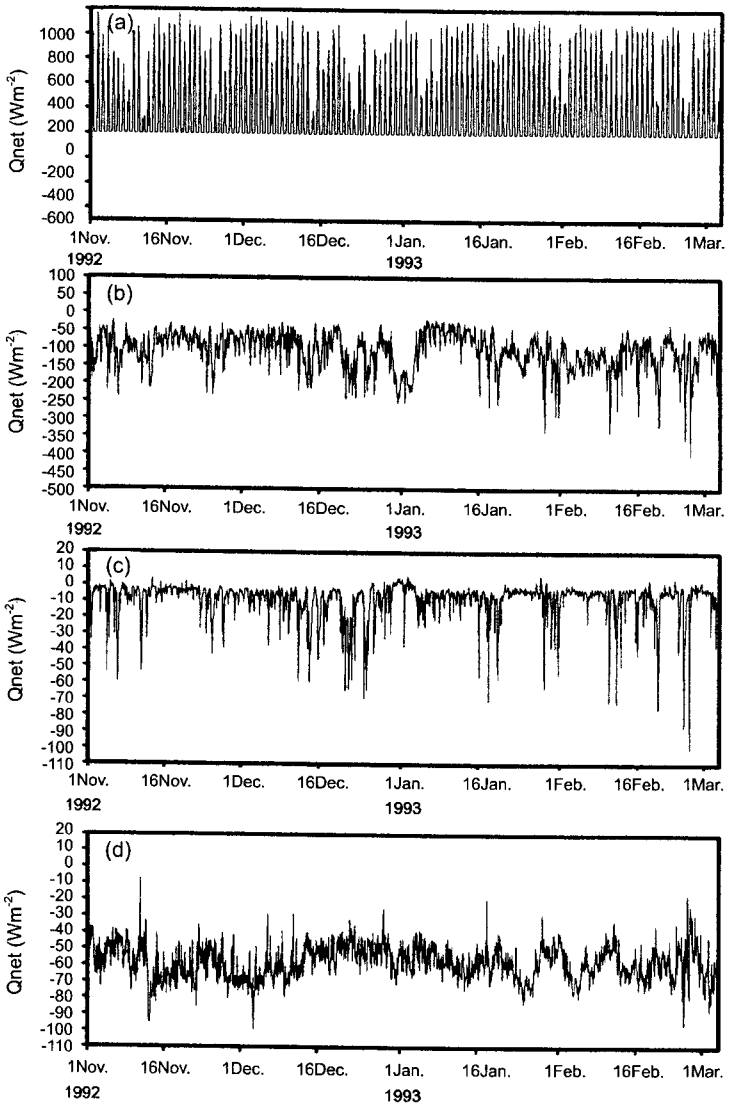

Fig. 2. Time series of components of the hourly net heat flux at IMET buoy during TOGA-COARE IOP: (a) net solar radiation, (b) latent heat flux, (c) sensible heat flux, and (d) net longwave radiation. Positive value is a gain for the ocean. Different y-axis scale for the components is used for clarity of presentation.

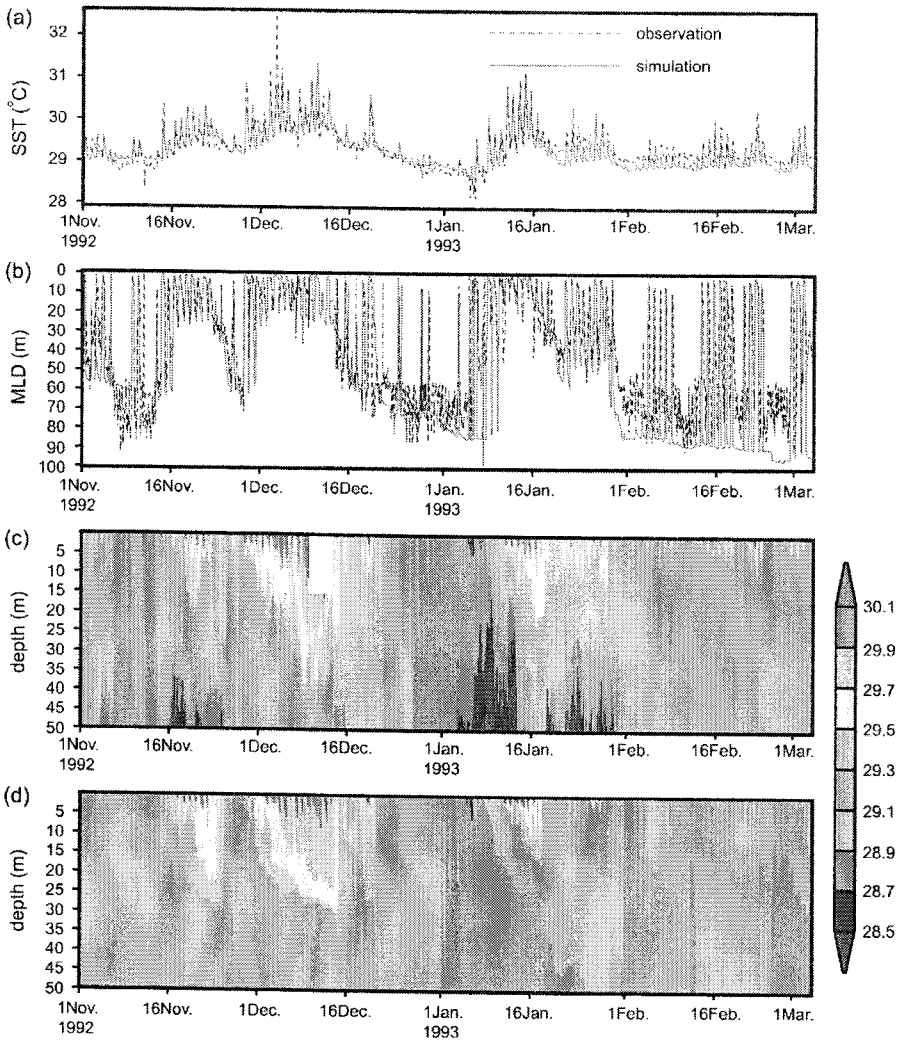

Fig. 3. Time series of (a) simulated SST, (b) simulated mixed layer depth, (c) observed subsurface temperature, and (d) simulated subsurface temperature. The observed SST in (a), and calculated mixed layer depth from observed temperature profiles in (b) are also shown by short-dashed black curves. The subsurface temperatures above 15 m were not observed around 11 Dec. 1992, denoted by a white box in (c).

shoaling and subsequent surface cooling/deepening, as seen in Figs. 3a and b.

The model successfully reproduces much of the observed SST variability including the amplitude of the daily cycles. The model SST deviates from the observed SST during the periods when either advection or undetermined processes are affecting variability (early November 1992 and after mid-January 1993), as pointed out by Anderson *et al.* (1996) and Li *et al.* (1998). A striking difference between the model and observations is seen after 16 January 1993; the model SST is continuously lower than the observed SST by up to 0.3°C. This cold-biased SST in the model arises because the model MLD is deeper than the observed one, which will be explained in detail below. This period coincides with the time when the residual temperature and salinity are relatively high, so the one-dimensional heat budget is not closed (Fig. A1 in Anderson *et al.* 1996 and Fig. 1 in Li *et al.* 1998).

The rms difference and the linear correlation coefficient between the observed and simulated SST are approximately 0.21°C and 0.89, respectively, indicating the overall good performance of the new mixed-layer model in simulating the SST. By comparison, Li *et al.* (1998) reported respective values of 0.28°C and 0.80.

The evolutions of the subsurface temperature in the

observation and simulation are shown in Figs. 3c and d. The evolution of the vertical temperature profile is reproduced quite well, although the warming around 16 January 1993 is limited to shallower depths (20 m) than observed. The one important feature that the model fails to reproduce is the appearance of a relatively low subsurface temperature (below 29.7°C) around 16 Nov. 1992 and from 1 Jan. until 1 Feb. 1993. This may be related to an internal tide or horizontal advection (Anderson *et al.* 1996).

The model MLD (Fig. 3b) closely follows the observed MLD; it deepens to 80-90 m during rain events (15 Dec. 1992-2 Jan. 1993), while it is trapped within the top 12 m during the late restratification period (5-15 Jan. 1993) after a westerly wind burst. Furthermore, the diurnal variation of the MLD under clear-sky conditions is also well reproduced, compared with observations; it is shallow during daytime heating and deep during nighttime cooling.

After 1 Jan. 1993, there is a significant difference when the MLD is deeper than about 70 m. The model MLD is approximately 20 m deeper than the observed MLD when the MLD becomes large after 1 Jan. 1993. This failure can be explained as follows. In the observations, the cold subsurface water below 28.7°C (Fig. 2c) results in strong stable stratification, thereby preventing the mixed layer from deepening below the depth of the cold water. The model fails to reproduce the cold subsurface water, and therefore the simulated mixed-layer deepening is not limited to the depth of the cold water. Accordingly, the model SST is about 0.3°C lower than the observed SST, because the heat from the surface is distributed within a larger mixed-layer depth than the observed values. This result shows the importance of proper representation of the subsurface water temperature, which can affect mixed-layer deepening and thus the SST.

Fig. 4 compares the simulated SSS at 2 m with the observed values. The simulated SSS deviates significantly from the observed SSS, and the difference reaches 1.4 psu around Jan. 16, 1993. It has been shown that the one-dimensional heat and salt budgets have the largest residuals during this time (Anderson *et al.* 1996; Li *et al.* 1998). The difference is especially large during heavy rainfall (15 Dec. 1992-2 Jan. 1993) and the subsequent restratification period (5-15 Jan. 1993). The simulated SSS at 2 m decreases during westerly wind bursts (15 Dec. 1992-2 Jan. 1993), owing to the relatively heavy rainfall, while the observed salinity does not show a clear decrease, indicating that other processes, such as advection or the entrainment of saline water into the mixed layer, are involved (Anderson *et al.* 1996; Li *et al.* 1998; Clayson and Kantha 1999). Based on the results of experiments with and without entrainment in the bulk mixed-layer model of Adamec *et al.* (1981), Li *et al.* (1998) suggested that the entrainment process significantly reduces the low-salinity bias during heavy rainfall by entraining saline water into the mixed layer. The entrainment process, however, increases the mixed-layer temperature, thereby causing a weaker cooling of the SST in the simulation than in observations during heavy rainfall, by entraining warm water below the mixed layer into the mixed layer, which is evident in their Fig. 3a. Clayson and Kantha (1999) also attributed the significant departure of the SSS from the observed value to the fact that their one-dimensional turbulence closure model ignored upwelling/downwelling processes.

To investigate the detailed response of the upper ocean to external forcing, SST, MLD, and the subsurface temperature are plotted in Figs. 5 and 6 during a westerly wind burst with heavy rainfall (15 Dec. 1992-2 Jan. 1993) and the subsequent restratification (5-15 Jan. 1993).

During the westerly wind burst with heavy rainfall, SST, MLD, and the subsurface temperature are well reproduced. In particular, the SST decrease of about 0.3°C is successfully simulated, which is clearly an improvement over previous simulations (Anderson *et al.* 1996; Sui *et al.*

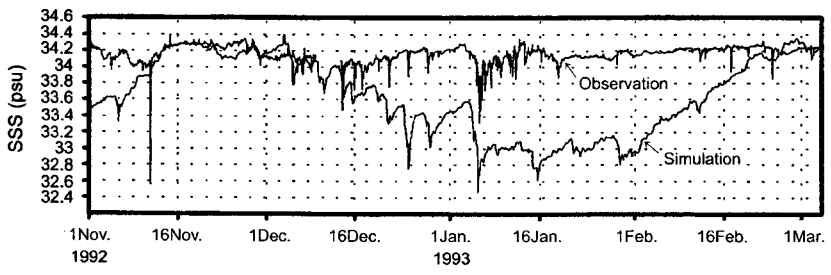

Fig. 4. Simulated and observed SSS at 2 m during the IOP.

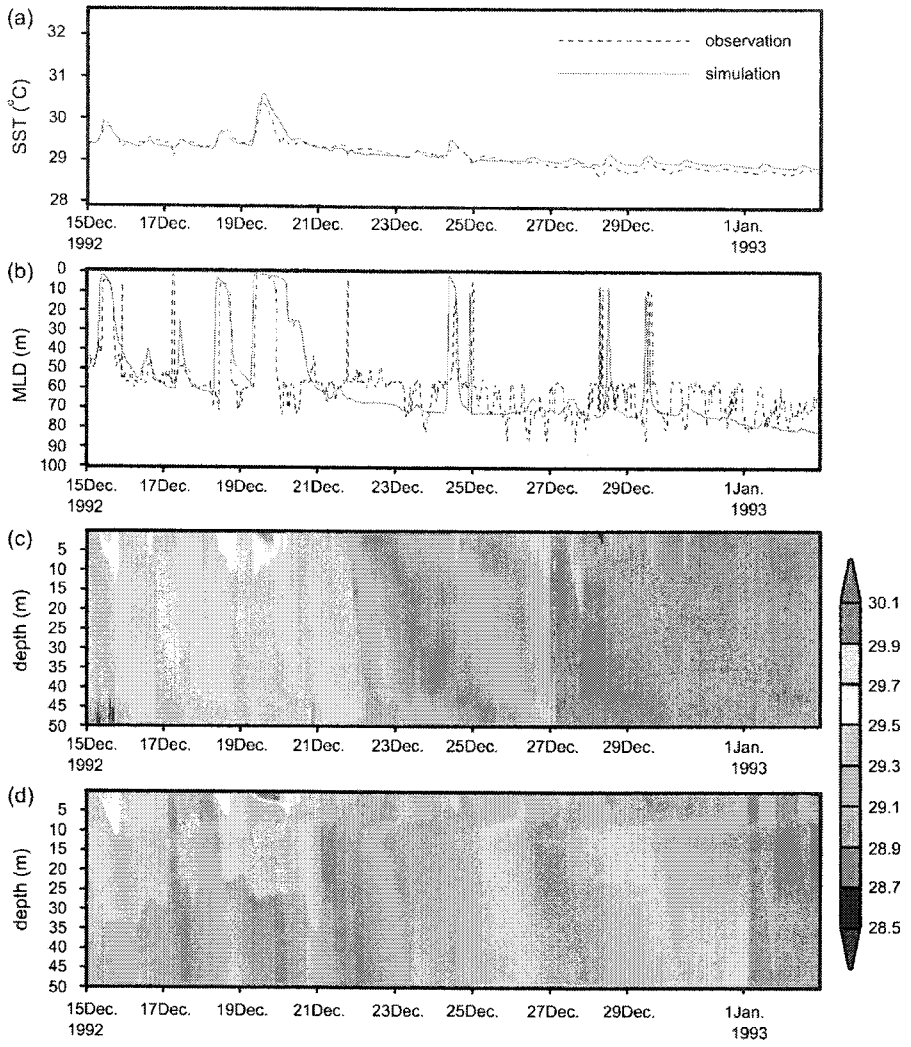

Fig. 5. Same as Fig. 3 except for during the westerly wind burst (15 Dec. 1992-2 Jan. 1993).

1997; Li *et al.* 1998). Previous simulations using bulk mixed-layer models suffered from relatively slow SST cooling during westerly wind bursts, as pointed by Li *et al.* (1998), which presumably resulted from insufficient mixing due to neglect of TKE production by vertical shear in the bulk mixed-layer models. The observed MLD is relatively deep (50-80 m) due to both strong wind mixing and negative heat flux and freshwater flux.

During the subsequent restratification, the simulation shows a rapid rise in the SST and shoaling of the MLD after 9 Jan. 1993. The mixed layer does not deepen below 15 m after 11 Jan. 1993. Accordingly, the SST continues to increase, to around 31°C, due to strong solar heating and weak wind. Warming at the subsurface after 13 Jan. 1993 is limited to depths shallower than the observed depths, which needs further investigation.

Fig. 7 shows the distribution of the model turbulent kinetic energy (TKE) and frictional velocity during a westerly wind burst and the subsequent restratification period. The model TKE is relatively high during the westerly wind burst, which causes deepening of the mixed layer during that period. The TKE is relatively low during the subsequent restratification period, resulting in the shallow MLD. This result suggests that the model TKE is highly correlated with the frictional velocity during these periods.

5. Summary and conclusion

The response of the mixed layer to local forcing in the western Pacific warm pool region during the TOGA-COARE IMET IOP was investigated using a one-

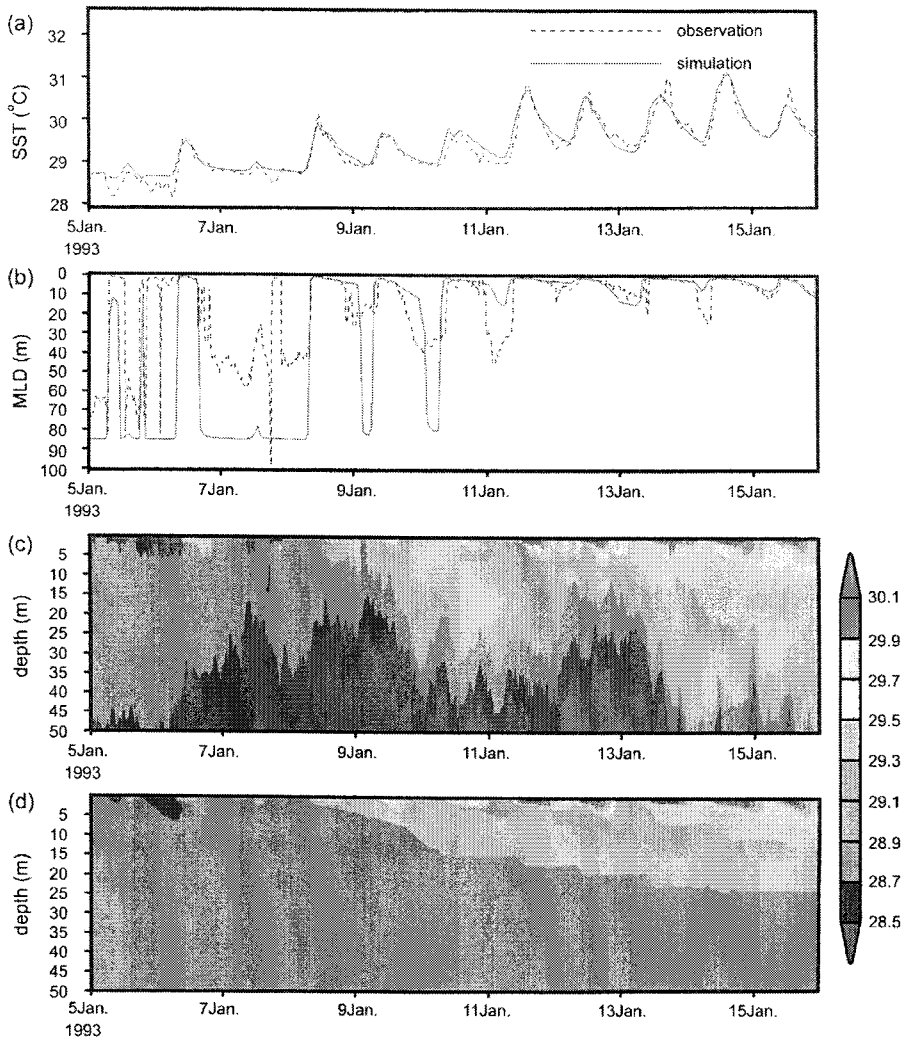

Fig. 6. Same as Fig. 3 except for during the subsequent restratification (5-15 Jan. 1993).

dimensional turbulence closure model based on Noh and Kim (1999). The mixed-layer model reproduced both the observed diurnal and intraseasonal variation in the upper ocean in the warm pool region. Furthermore, simulation of the cooling trend of SST during a westerly wind burst with heavy rainfall was better than in previous simulations (Anderson *et al.* 1996; Sui *et al.* 1997; Li *et al.* 1998). The root mean square difference and the linear correlation coefficient between the observed and simulated SST were approximately 0.21°C and 0.89, respectively, indicating the overall good performance of the new mixed-layer model in simulating the SST. On the other hand, warming at the subsurface after 13 Jan. 1993 was limited to depths shallower than the observation depths, which needs further investigation.

The simulated SSS departed significantly from the observed SSS, especially during the westerly wind burst and subsequent restratification period. For instance, around 16 Jan. 1993, the simulated SSS is about 1.4 psu lower than the observed value. This problem of SSS departure also arose in previous models (Anderson *et al.* 1996; Sui *et al.* 1997; Li *et al.* 1998; Clayson and Kantha 1999), and might be because these models neglect other processes controlling the SSS, such as downwelling/upwelling or advection.

The one-dimensional model simulation of the mixed layer in the warm pool also has a limited ability to simulate the subsurface thermal structure. This failure is apparent in the simulation of the subsurface water from 1 Jan. until 1 Feb. 1993, which results in a deeper mixed layer (about 20 m) in the simulation than was observed, and consequently the simulated SST is about 0.3°C lower

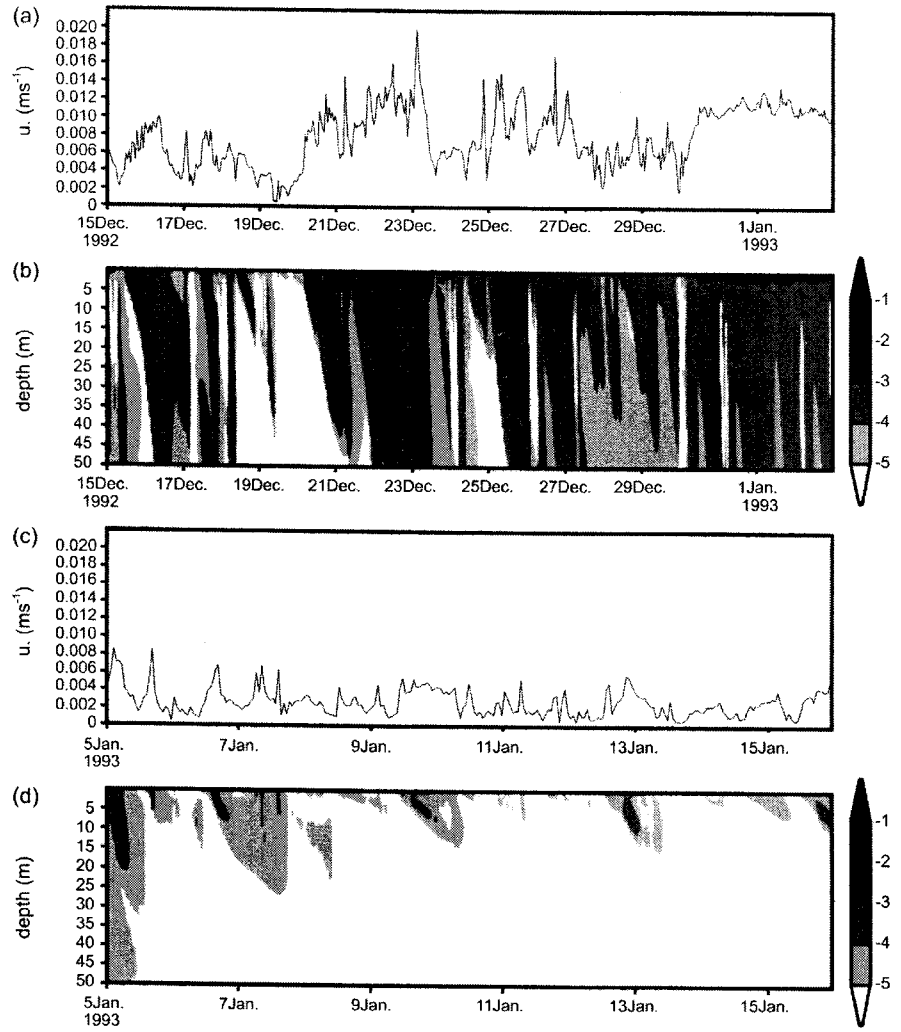

Fig. 7. Time series of (a) frictional velocity and (b) model TKE ($\log_{10}$ TKE) during the westerly wind burst, and (c) frictional velocity and (d) model TKE ($\log_{10}$ TKE) during subsequent restratificatin period.

than the observed SST after 16 January 1993. This shows the importance of proper representation of subsurface water temperature in simulating the mixed-layer depth and SST.

In the future, it will be necessary to investigate the roles of three-dimensional processes, such as advection and entrainment, in the response of the upper ocean in the warm pool.

Acknowledgements

The authors thank Drs. Kyung-Tae Jung, Jung-Bae An, Kyung-Il Chang for constructive comments which improved the manuscript significantly. This research is supported by the Ministry of Education (Brain Korea 21 Project), Ministry of Environment (Echo-Technopia 21 Project), and Ministry of Science and Technology/ Ministry of Defence (Virtual Ocean Project).

References

Adamec, D., R.L. Elsberry, R.W. Garwood, Jr., and R.L. Haney. 1981. An embedded mixed-layer ocean circulation model. *Dyn. Atmos. Oceans*, 6, 69-96.

Anderson, S.P., R.A. Weller, and R.B. Lukas. 1996. Surface buoyancy forcing and the mixed layer of the western Pacific warm pool: Observations and 1D model results. *J. Clim.*, 3056-3085.

Barnier, B. 1998. Forcing the ocean. p. 45-80. In: *Ocean Modeling and Parameterization*, eds. by E.P. Chassignet and J. Verron. Kluw. Acad. Pub.

Clayson, C.A. and L.H. Kantha. 1999. Turbulent kinetic energy and its dissipation rate in the equtorial mixed layer. *J. Phys. Oceanogr.*, 29, 2146-2166.

Craig, P.D. and M.L. Banner. 1994. Modeling wave-enhanced turbulence in the oceanic surface layer. *J. Phys. Oceanogr.*, 24, 2546-2559.

Cronin, M.F. and M.J. McPhaden. 1997. The upper ocean heat balance in the western equatorial Pacific warm pool during September-December 1992. *J. Geophys. Res.*, 8533-8553.

Davies, A.M. and J.E. Jones. 1988. Modeling turbulence in shallow sea regions. p. 63-76. In: *Small-scale Turbulence and Mixing in the Ocean*, eds. by J. C.J. Nihoul and B.M. Jamart. Elsevier, New York.

Jerlov, N.G. 1968. *Optical Oceanography.* Elsevier, 194 p.

Li, X., C.-H. Sui, D. Adamec, and K.-M. Lau. 1998. Impacts of precipitation in the upper ocean in the western Pacific warm pool during TOGA-COARE. *J. Geophys. Res.*, 5347-5359.

Martin, P.J. 1985. Simulation of the mixed layer at OWS November and Papa with several models. *J. Geophys. Res.*, 90, 903-916.

Mellor, G.L. and T. Yamada. 1982. Development of a turbulent closure model for geophysical fluid problems. *Rev. Geophys*, 20, 851-875.

Niiler, P.P. and E.B. Kraus. 1977. One dimensional models of the upper ocean. p. 143-172. In: *Modeling and Prediction of the Upper Layers of the Ocean*, ed. by E.B. Kraus. Pergamon, Tarrytown, N.Y.

Noh, Y. 1996. Dynamics of diurnal thermocline formation in the oceanic mixed layer. *J. Phys. Oceanogr.*, 26, 2183-2195.

Noh, Y. and H.J. Kim. 1999. Simulation of temperature and turbulence structure of the oceanic boudary layer with the improved near-surface process. *J. Geophys. Res.*, 104, 15621-15634.

Palmer, T.N. and D.A. Mansfield. 1984. Response of two atmospheric general circulation models to sea surface temperature anomalies in the tropical east and west Pacific. *Nature,* 483-485.

Paulson, C.A. and J.J. Simpson. 1977. Irradiance measurements in the upper ocean. *J. Phys. Oceanogr.*, 7, 952-956.

Phillips, O.M. 1977. *The Dynamics of the Upper Ocean.* 2nd ed. , Cambridge Univ. Press, New York.

Price, J.F., R. Weller, and R. Pinkel, 1986. Diurnal cycling: Observations and models of upper ocean response to diurnal heating, cooling and wind mixing. *J. Geophys. Res.*, 91, 8411-8427.

Sui, C.-H., X. Li, K.-M. Lau, and D. Adamec. 1997. Multi-scale air-sea interactions during TOGA COARE. *Mon. Weather Rev.*, 448-462.

Weller, R.A. and S.P. Anderson. 1996. Surface meteorology and air-sea fluxes in the western equatorial Pacific warm pool during TOGA-COARE. *J. Clim.*, 9, 1959-1990.

Received Nov. 28, 2001
Revised May 29, 2002
Accepted Jun. 24, 2002